Supporting Information

Yadid et al. 10.1073/pnas.0912616107

SI Text

Supplementary Methods. ***Directed evolution toward higher expression.*** As a first step, additional aminoacids at N and C termini that resulted from the incremental truncation procedure were removed, to produce the "net" variants. The four additional C terminus aminoacids (Arg-Val-Thr-Lys) from Lib1-B7 and Lib2-D2 were replaced by a stop codon and a *NotI* restriction site by amplification with the primers *B7-short-bc* (5′-ATAGTTTAGCGGCCGCTTAATCCTGGTTAGACACCGGCGGTAATGC) and *D2-Polished-bc* (ATAGTTTAGCGGCCGCTTAGCCGCCGCTTCCAA-TTTC). To remove the additional aminoacids (Val-Asp) at the N terminus of Lib1-B7, and maintain the *NcoI* site, a small combinatorial library was prepared using the primer *B7 short for* (CATGCCATGGNNAAAGGGACGCCGCCTACTC). Screening for mucin binding indicated that the having Glu right after the first Met yielded the highest activity. In Lib2-D2, the additional N terminus aminoacids (Val-Glu) were removed using the primer *D2 Polished for* CATGCCATGGGCGGCTGGTCTAACTTC. The resulting net variants were subjected to three to four rounds of random mutagenesis and screened by ELLA on mucin-coated plates.

Random mutagenesis by error-prone PCR. Mutagenesis was performed by error-prone PCR and the conditions were adjusted to give an average of one nonsynonymous mutation per gene. The open reading frames of the net variants Lib1-B7 and Lib2-D2 were cloned in to pETtr, yielding pETtrB7 or pETtrD2, respectively, and were mutated using 20–200 ng/ml plasmid templates and three different nucleotide bias ratios: 1:5, 1:10, 1:20 dG/TTP to dA/CTP. PCRs were performed in reaction buffer (BioLine), dG/TTP 1–4 mM, dA/CTP 0.2 mM, $MgCl_2$ 3.6–9.6 mM, $MnCl_2$ 0.125 mM, oligonucleotides primers *pETtr-for-out* (AATACGACTCACTATAGGGGAATTGTG, 0.5 μM) and *pETtr-bc-out* (TTTAGAGGCCCCAAGGGGTTATGC, 0.5 μM), and 1 unit of BioTaq (Bioline) (2 min at 94 °C, followed by 20–30 cycles of 30 s at 94 °C, 30 s at 56 °C and 4 min at 72 °C, with a final 7 min at 72 °C). The amplified DNA fragments were treated with *DpnI* to remove the plasmid template and then subjected to a second PCR in reaction buffer (BioLine), dNTPs 0.2 mM, $MgCl_2$ 2 mM, oligonucleotides primers 0.5 μM each (*pETtr-for-in* ATTGTGAGCGGATAACAATTCCCCTC, and *pETtr-bc-in* TTAGCAGCCGGATCTCAGTGG) and 1 unit of BioTaq (Bioline) (2 min at 94 °C, followed by 25 cycles of 30 s at 94 °C, 30 s at 56 °C and 1 min at 72 °C, with a final 7 min at 72 °C). Alternatively, error-prone PCR was performed by a single PCR on 20–200 ng plasmid template using Genemorph II© mutagenesis kit (Stratagene), in the manufacturer's reaction buffer (Stratagene), dNTPs 0.2 mM, *pETtr-for-out* 0.5 μM, *pETtr-bc-out* 0.5 μM, and 1 unit of mutazyme© (2 min at 94 °C, followed by 20–30 cycles of 30 s at 94 °C, 30 s at 56 °C and 1 min at 72 °C, with a final 7 min at 72 °C). The mutated PCR fragments were cloned back into pETtr using *NcoI* and *NotI* and transformed to *Escherichia coli* DH5-α cells and the library plasmid DNAs were extracted.

Enzyme linked lectin assay (ELLA) screens. Library plasmid DNAs were transformed into *E. coli* BL21 (DE3) cells for expression and screening for their ability to bind glycoproteins. The transformed cells were plated on agar plates supplemented with 100 μg/ml amppicilin and 1% glucose. Individual colonies were picked and grown in 96-well plates containing 500 μl LB supplemented with 100 μg/m amppicilin. This was shaken overnight at 37 °C. The starters was then transferred into new 96 plates containing LB (500 μl) supplemented with ampicillin (100 μg/ml) and grown to an $OD_{(600nm)}$ of 0.6. Isopropyl β-D-1-thiogalactopyranoside (IPTG) was added to a final concentration of 0.4 mM and the culture shaken for 4.5 h at 37 °C. Cells were harvested at 2500 × *g* for 20 min and the bacteria pellet were frozen at −70 °C overnight. Bacteria pellet were resuspended in lysis buffer (200 μl) containing 20 mM Tris pH 7.5, 150 mM NaCl (TBS), 0.2 mg/ml lysozyme, 1:50,000 benzonase nuclease® (Novagen) and supplemented with complete© protease inhibitor (Roche). Cell lysates were incubated on mucin (porcine stomach mucin type II from sigma) coated plates (100 μl of 5 μg/ml mucin in PBS) with 2%BSA for 1 h and washed 3 times with PBS-0.5% tween. The volume of lysate applied to the plates was decreased as the process of directed evolution advanced to increase the stringency (5 μl in the first round and 0.005 μl at the fourth round). Proteins were detected using polyclonal rabbit anti tachylectin-2 antibodies (antibodies were produced in our institute after three immunizations with recombinant tachylectin-2), followed by goat-anti-rabbit HRP antibodies and the TMB substrate (Dako).

Protein production and purification. Lectin variants were expressed in BL-21(DE-3) from pET32b (Novagen) vector from which the Trx fusion protein and peptide tags were removed (pET32-tr), resulting in the expression of an unaltered protein. A starter was grown from a single colony in LB medium (5 ml) supplemented with glucose (1%) and ampicillin (100 μg/ml) at 37 °C overnight. This starter was then transferred into LB (500 ml) supplemented with ampicillin (100 μg/ml) and grown to $OD_{(600nm)}$ of 0.6. Isopropyl β-D-1-thiogalactopyranoside (IPTG) was added to a final concentration of 0.4 mM and the culture shaken for 4.5 h at 37 °C. Cells were harvested at 2500 × *g* for 20 min and the bacteria pellet were resuspended in lysis buffer (50 ml) containing 20 mM Tris pH 7.5, 150 mM NaCl (TBS) supplemented with one tablet of Complete© protease inhibitor (Roche). Cells were then sonicated on ice at 40% intensity (Branson Sonicator Cell Disrupter model 130, Branson Ultrasonics, Danbury, CT) six times for 30 sec with 30 sec intervals, and then centrifuged 20 min at 18,000 × *g*, at 4 °C. N-Acetyl-D-Glucosamine Agarose (1 ml) (Sigma) was added to the supernatant and agitated gently at 4 °C for 16 h. The agarose beads were separated and washed with 25 volumes of TBS. For elution, TBS (1 ml) containing 250 mM N-Acetyl-D-Glucosamine (GlcNAc) was added to the beads and left to stand at room temperature. After 30 min, the protein was eluted with additional volumes of TBS with 250 mM GlcNAc until no protein was observed in the elution judged by absorption at 280 nm. Relevant fractions as judged by $OD_{(280\,nm)}$ were pooled and dialyzed six times against TBS to remove GlcNAc. Selenomethionine Lib1-B7-18 was produced using the Van Duyne *et.al* protocol (1).

Isothermal titration calorimetry. Titration calorimetry experiments were performed using the Microcal (Northampton, MA) iTC-200 microcalorimeter. All titrations were performed in phosphate buffered saline (PBS, pH 7.4) containing 150 mM NaCl. Aliquots of 1.5 μL of the carbohydrate solution in the same buffer were added at 120 sec intervals to the lectin solution present in the calorimeter cell. The sugar concentration in the 40 μl syringe was ∼100 times higher than the protein concentration. The temperature of the cell was kept at 25 ± 0.1 °C. Data from a control experiment performed via identical injections of monosaccharide

into the cell containing only a buffer were negligible and therefore was not subtracted from the dataset. Integrated heat effects were analyzed by nonlinear regression using a single site binding model (Microcal Origin 7). The number of sites (n) was kept constant, and fitted data yielded the association constant (K_a) and the enthalpy of binding (ΔH). Other thermodynamic parameters, i.e., changes in free energy (ΔG) and entropy (ΔS), were calculated from the equation: $\Delta G = \Delta H - T\Delta S = RT \ln K_a$, where T is the absolute temperature and $R = 8.314$ J mol^{-1} K^{-1}.

Crystallization, data collection, and refinement. Crystals of Lib1-B7-18 were obtained by the hanging drop method. Selenomethionine Lib1-B7-18 crystals were grown from a solution of 100 mM Bis-Tris pH = 5.5, 10 mM GlcNAc, 0.2 M lithium chloride, and 19% PEG 3350. Crystals formed in a space group $P3_2$ with cell constants $a = b = 80.56$ Å, $c = 170.68$ Å, and contain ten monomers in the asymmetric unit cell with Vm of 2.66 Å^3/Dalton. The data to 2.5 Å resolution from a single crystal were collected at the European Synchrotron Radiation Facility (ESRF) beam line ID14-4. The crystals of Lib2-D2-15 obtained under oil by the microbatch method using the Oryx6 robot (Douglas Instruments Ltd., East Garston, Hungerford, Berkshire, UK), diffracted to 2.5 Å resolution. Lib2-D2-15 crystals were grown from a solution of 100 mM HEPES pH = 7.0, 10 mM GlcNAc, 0.2 M magnesium chloride, and 20% PEG 6000. Crystals formed in a space group $C2$ with cell constants $a = 125.56$ Å, $b = 56.42$ Å, $c = 86.31$ Å, and $\beta = 122.90°$ and contain five monomers in the asymmetric unit cell with Vm of 2.41 Å^3/Dalton. A complete dataset up to 2.5 Å was collected on a Rigaku R-AXIS IV++ imaging plate area detector mounted on a Rigaku RU-H3R generator with CuKα radiation focused by Osmic confocal mirrors. The diffraction data were indexed and integrated using the program, HKL2000 (2). Integrated intensities were scaled using the program SCALEPACK (2). The structure factor amplitudes were calculated using TRUNCATE from the CCP4 program suite (3). The structures of Lib2-D2-15 and Lib1-B7-18 were determined by molecular replacement using the known structure of wilde-type tachylectin-2 (PDB code 1TL2 (4)) as a starting model without the need for a SeMet MAD experiment. The refinement was carried out using the program, CCP4/Refmac5 (5). The model was used to built the electron density maps ($2F_{obs} - F_{calc}$ and $F_{obs} - F_{calc}$) using the program COOT (6). Water molecules were built into peaks greater than 3σ in the $F_{obs} - F_{calc}$ maps. Finally, the Lib2-D2-15 and Lib1-B7-18 models were evaluated with the program MolProbity. (7) The details of the refinement statistics of the Lib2-D2-15 and Lib1-B7-18 structures are presented in Table S2. The coordinates and structure factors for the Lib2-D2-15 and Lib1-B7-18 structures have been deposited in the RCSB PDB under accession No. 3KIH and 3KIF respectively. All figures depicting structures were prepared using PyMOL (DeLano Scientific LLC).

Mass spectrometry. In order to define the subunit stoichiometry of the tachylectin-2 variants, *Lib1-B7-10, Lib1-B7-18, Lib2-D2-6*, and *Lib2-D2-15*, structural mass spectrometry analysis was carried out on a nanoflow ESI QSTAR Elite (Sciex) mass spectrometer modified for transmission and isolation of high mass ions (8, 9). Prior to MS analysis 25 μl of up to 100 μM sample was buffer-exchanged into 0.5 M ammonium acetate (pH 7.5) using Micro Biospin columns (BioRad), and 1.5 μl aliquots were introduced via nanoflow capillaries prepared in-house. Throughout the analysis conditions within the mass spectrometer were adjusted to preserve noncovalent interactions. The following experimental parameters were used: capillary voltage up to 1.2 kV, declustering potential up to 150 V, focusing potential 250 V, second declustering potential 55 V, and focusing rod offset ranging from 20 to 100 V, MCP 2350 V. All spectra were calibrated externally by use of a solution of cesium iodide (100 mg/mL). Spectra are shown here with minimal smoothing and without background subtraction.

1. G. D. Van Duyne, R. F. Standaert, P. A. Karplus, S. L. Schreiber & J. Clardy (1993) Atomic structures of the human immunophilin FKBP-12 complexes with FK506 and rapamycin. *J Mol Biol* 229:105–124.
2. Z. Otwinowski & W. Minor (1997) Processing of x-ray diffraction data collected in oscillation mode. *Method Enzymol* 276:307–326.
3. G. S. French & K. S. Wilson (1978) On the treatment of negative intensity observations. *Acta Crystallogr A*A34:517–552
4. H. G. Beisel, S. Kawabata, S. Iwanaga, R. Huber & W. Bode (1999) Tachylectin-2: Crystal structure of a specific GlcNAc/GalNAc-binding lectin involved in the innate immunity host defense of the Japanese horseshoe crab Tachypleus tridentatus. *EMBO J* 18:2313–2322.
5. G. N. Murshudov, A. A. Vagin & E. J. Dodson (1997) Simplified error estimation a la Cruickshank in macromolecular crystallography. *Acta Crystallogr D* 53:240–255.
6. P. Emsley & K. Cowtan (2004) Coot: Model-building tools for molecular graphics. *Acta Crystallogr D* 60:2126–2132.
7. I. W. Davis et al. (2007) MolProbity: All-atom contacts and structure validation for proteins and nucleic acids. *Nucleic Acids Res* 35:W375–383.
8. I. V. Chernushevich & B. A. Thomson (2004) Collisional cooling of large ions in electrospray mass spectrometry. *Anal Chem* 76:1754–1760.
9. F. Sobott, H. Hernandez, M. G. McCammon, M. A. Tito & C. V. Robinson (2002) A tandem mass spectrometer for improved transmission and analysis of large macromolecular assemblies. *Anal Chem* 74:1402–1407.
10. I. Yadid & D. S. Tawfik (2007) Reconstruction of functional beta-propeller lectins via homo-oligomeric assembly of shorter fragments. *J Mol Biol* 365:10–17.
11. N. Okino et al. (1995) Purification, characterization, and cDNA cloning of a 27-kDa lectin (L10) from horseshoe crab hemocytes. *J Biol Chem* 270:31008–31015.

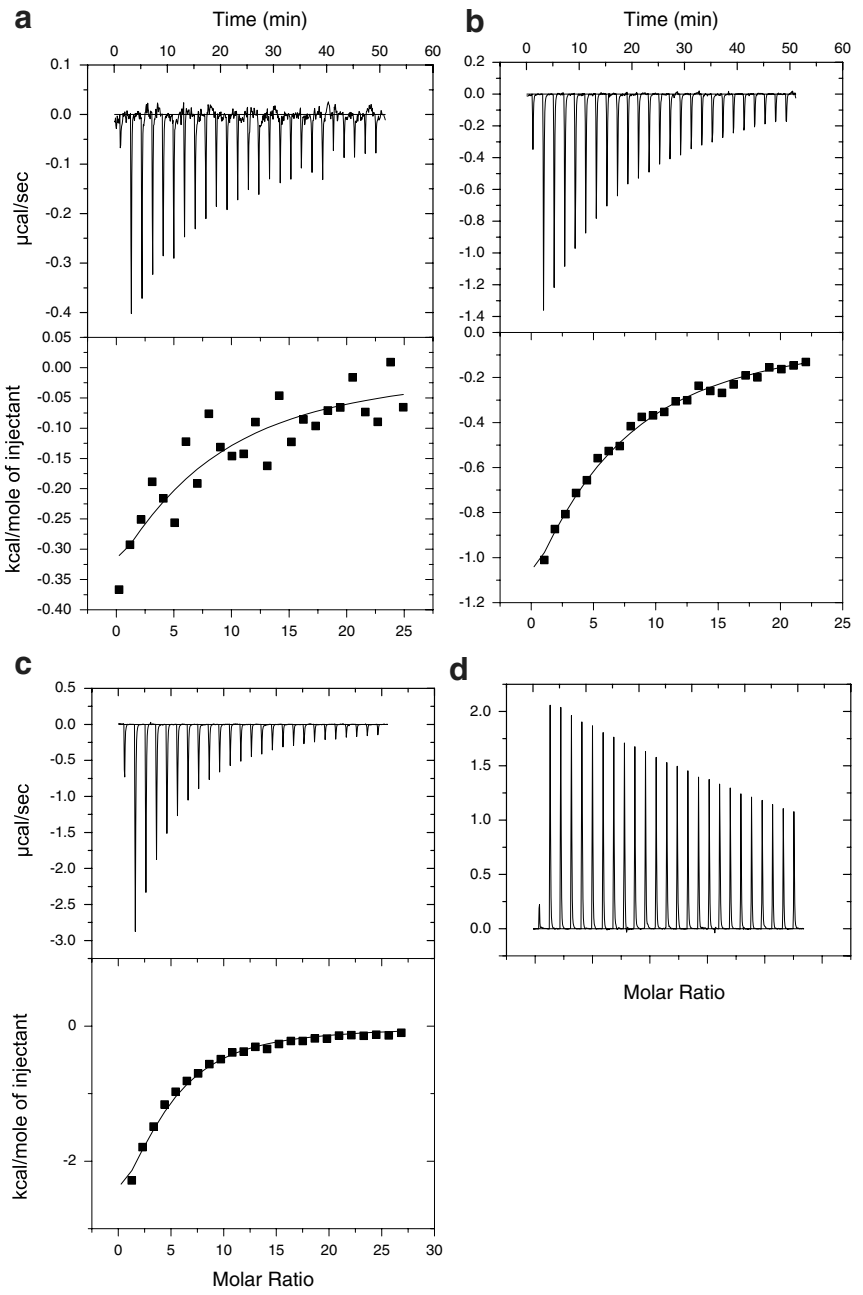

Fig. S1. Isothermal titration microcalorimetry. Binding of GlcNAc (0–10 mM) to tachylectin-2 (76 μM, *A*); Lib1-B7-18 (88 μM, *B*), and Lib2-D2-15 (72 μM, *C*), or of N-glucoseamine (GlcN, 0–10 mM) to Lib2-D2-15 (72 μM, *D*). Data were obtained from 25 automatic injections of 1.5 μl of GlcNAc or GlcN, into the lectin containing cell. Plots of the total heat release as a function of time for the titration are shown in the upper panel. The lower panels show the best least-squares fit for the obtained data using the instrument's software, while assuming that the number of sites (*n*) for the pentameric lectins Lib-1B7-18 and Lib2-D2-15 is 4, and for tachylectin-2 is 5. The results are summarized in Table S3. It should be noted that tachylectin-2 gave noisy data, possibly due to its tendency to aggregate at high concentrations. The fit gave an association constant (K_a) that is ~10-fold weaker than obtained by fluorescence quenching. The evolved lectins gave K_a values that are similar to the ITC value obtained for tachylectin-2, and 2-6-fold weaker values in comparison to the reported K_a value obtained by fluorescence quenching. It therefore seems that the affinity of individual sites remained similar, as suggested by the structures (Fig. S6). It should also be noted that the fit is not sufficiently stringent with respect to the number of sites. Introducing *n* values in the range of 1.5 up to 4 gave similarly good fits, and only values that span beyond this range gave significant deviations. This is likely to be because of having three floating parameters (*n*, K_a, and ΔH).

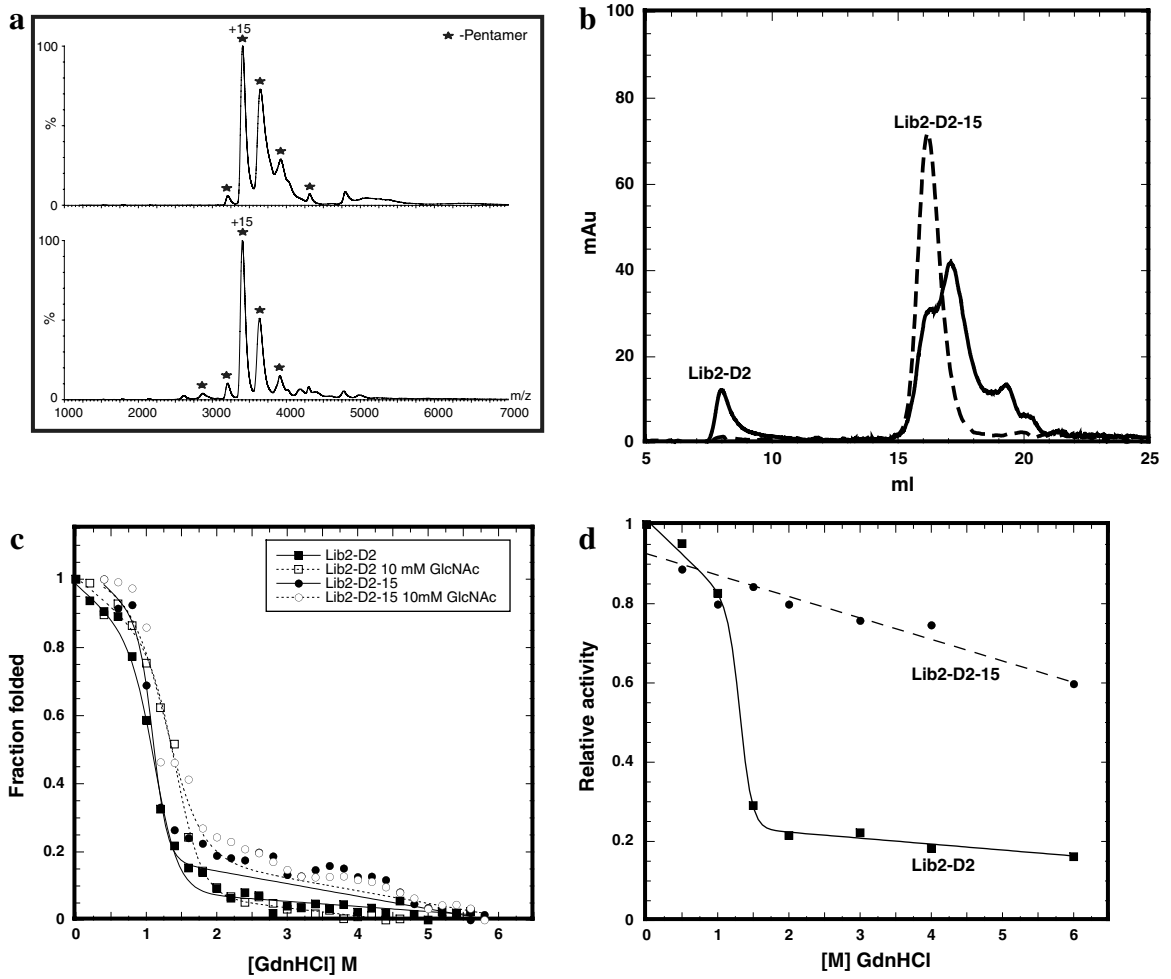

Fig. S2. Biophysical features of the pentameric lectin Lib2-D2-15. (*A*) Mass spectrometry of a variant from second round of evolution (Lib2-D2-6—upper spectrum) and the evolved variant Lib2-D2-15 (lower spectrum) were analyzed and confirmed that pentameric assembly is the main oligomeric state throughout all evolutionary rounds (see also Fig. S3). (*B*) Elution patterns Lib2-D2 and its evolved variant from a Superdex 200/30 gel filtration column. Lib2-D2 was eluted in five picks at: 8.03, 16.25, 17.15, 19.35 and 20.39 ml, presumably corresponding to high molecular weight aggregates, pentamers, tetramers, trimers and dimmers, respectively. Lib2-D2-15 was eluted as one pick at 16.23 ml corresponding to a pentamer. (*C*) Guanidinium hydrochloride (GdnHCl) denaturation curves in the absence or presence of the sugar ligand (GlcNac, 5 mM). Curves systematically deviated from the two-state model, and only apparent D_{50} values could be derived and were: 1.14 and 1.44 M for Lib2-D2 without and with the addition of 5 mM GlcNAc respectively and 1.1 and 1.27 M for Lib2-D2-15 without and with the addition of 5 mM GlcNAc. (*D*) Refolding as reported by binding activity. Lectins were unfolded using various concentrations of GdnHCl as indicated, and refolding was induced by diluting the denatured proteins into Phosphate Buffer Saline pH 7.4. The residual activity of the refolded lectins was than measured by ELLA on mucin-coated plated. Proteins were assayed in serial dilutions and the $E_{50\%}$ (50% of the maximum ELLA signal) were used to calculate residual activity, where the $E_{50\%}$ of 0 M GdnHCl is 1.

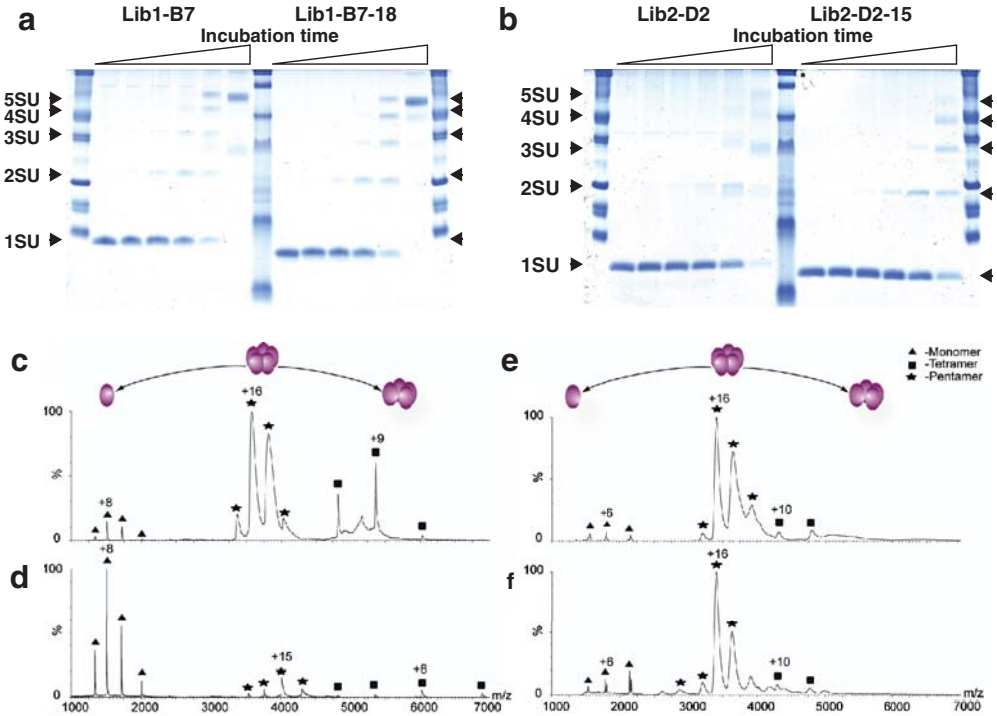

Protein	Theoretical monomer mass (Da)	Measured monomer mass (Da)	Theoretical tetramer mass (Da)	Measured tetramer mass (Da)	Theoretical pentamer mass (Da)	Measured pentamer mass (Da)
Lib1 -B7 -10	12,049	12,057 ± 1	48,195	48,212 ± 3	60,244	60,310 ± 21
Lib1 -B7 -18	12,026	12,036± 4	48,103	48,102 ± 6	60,129	60,134 ± 2
Lib2 -D2 -6	10,790 10,659 [a]	10,797 ± 1 10,666 ± 1	43,161 42,637 [a]	43,057 ± 2 42,773 ± 50	53,952 53,297 [a]	53,840 ± 13 53,371 ± 3
Lib2 -D2 -15	10,800 10,669 [a]	10,805 ± 1 10,674± 1.	43,201 42,677 [a]	43,146 ± 23 42,776 ± 55	54,002 53,347 [a]	54,040 ± 12 53,527 ± 13

[a] Mass calculated with the N-terminus methionine removed.

Fig. S3. Stoichiometry validation by cross-linking and structural mass spectrometry. Chemical cross-linking of the starting points and the evolved variants with 0.01% glutaraldehyde for increasing time points were performed as described in ref. 10. The reaction was stopped by the addition of $NaBH_4$ to a final concentration of 0.01 M, and the proteins were analyzed on 15% SDS-tricin gels. Black arrow tips indicate the number of cross-linked subunits (SU). (*A*) Lib1-B7 and its evolved variant Lib1-B7-18. (*B*) Lib2-D2 and its evolved variant Lib2-D2-15. (*C*) The spectra demonstrates the dissociation of the native pentameric form into a tetrameric complex in the range of 4, 500 m/z to 7, 000 m/z and monomeric subunits in the range of 1, 000 m/z to 2, 000 m/z in Lib1-B7-10. (*D*). Lib1-B7-18. (*e*). Lib2-D2-6 and (*f*) Lib2-D2-15. Table: Theoretical and measured masses of individual proteins and protein complexes observed in spectra of the evolved pentameric lectins.

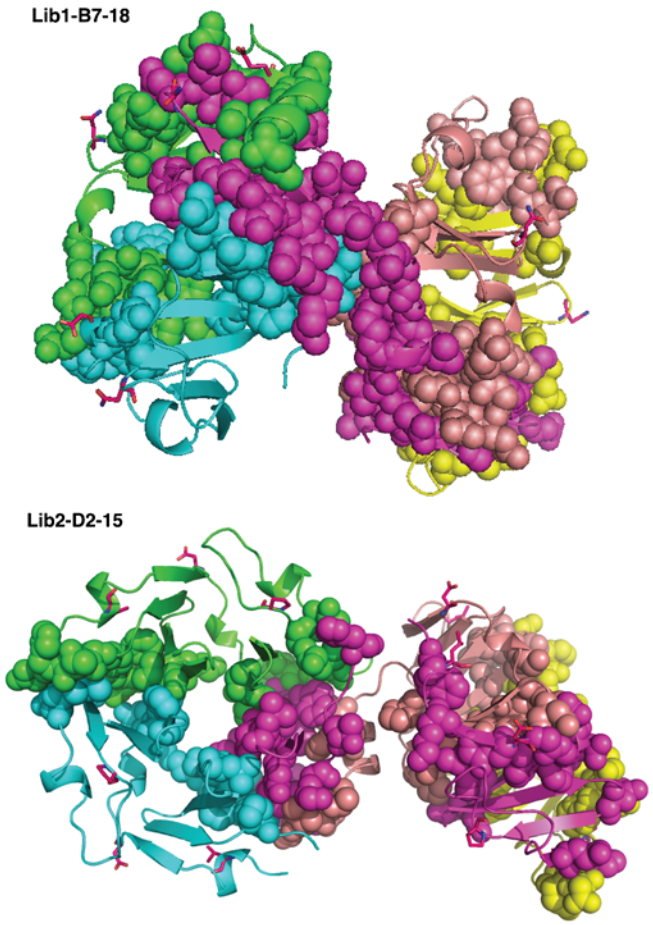

Fig. S4. New contacts between the oligomeric subunits. The bridging subinits are playing a crucial role in assembly and stabilization of the oligomeric lectins. Presented are the two-pentameric lectins: Lib1-B7-18 and Lib2-D2-15. The different subunits are colored as follow: Subunit A, green; B, cyan; C, magenta; D, yellow; and E, wheat. Residues contribute to the interaction between the subunits are shown as spheres, and residues that were mutated during rounds of mutagenesis are presented as sticks.

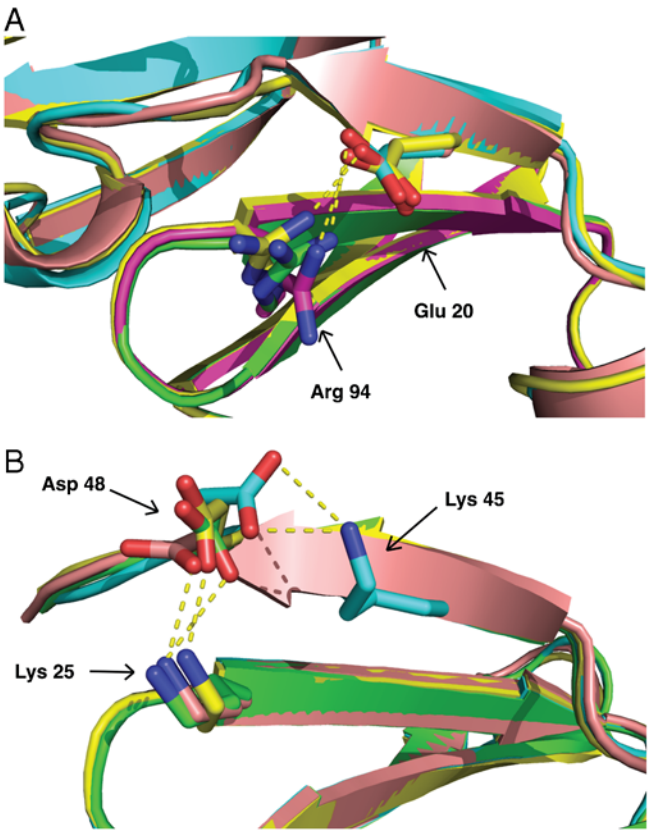

Fig. S5. Structural details of the mutations. (*A*) The newly formed interaction of Glu20 (Lys20 in the wild-type derived fragment Lib1-B7) with Arg 94 in Lib1-B7-18. (*B*) The newly formed interaction of Asp48 (Asn in the wild-type derived fragment Lib2-D2) with Lys 45 or Lys 25 in Lib2-D2-15.

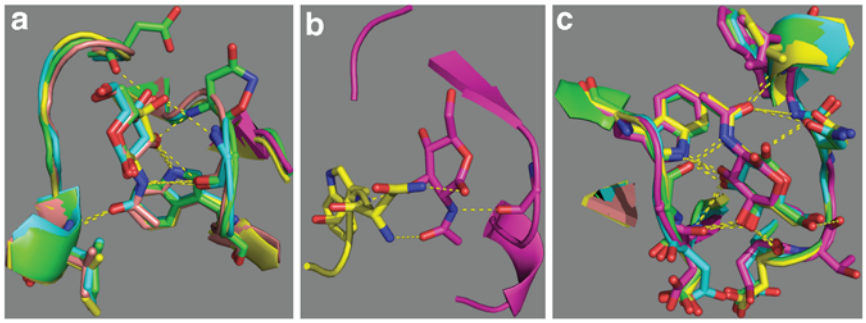

Fig. S6. The sugar binding sites of the evolved lectins colored by subunits as in Fig. S3. (*A*) In Lib1-B7-18, there are two different classes of binding sites, the first class is observed within intact subunits, and these sites perfectly align with the wild-type tachylectin-2 binding sites. (*B*) The second class of binding sites is formed at the subunit interface and is markedly different from the wild-type binding sites. (*C*) In Lib2-D2-15 one class of functional binding sites is observed that is essentially identical to those observed in tachylectin-2.

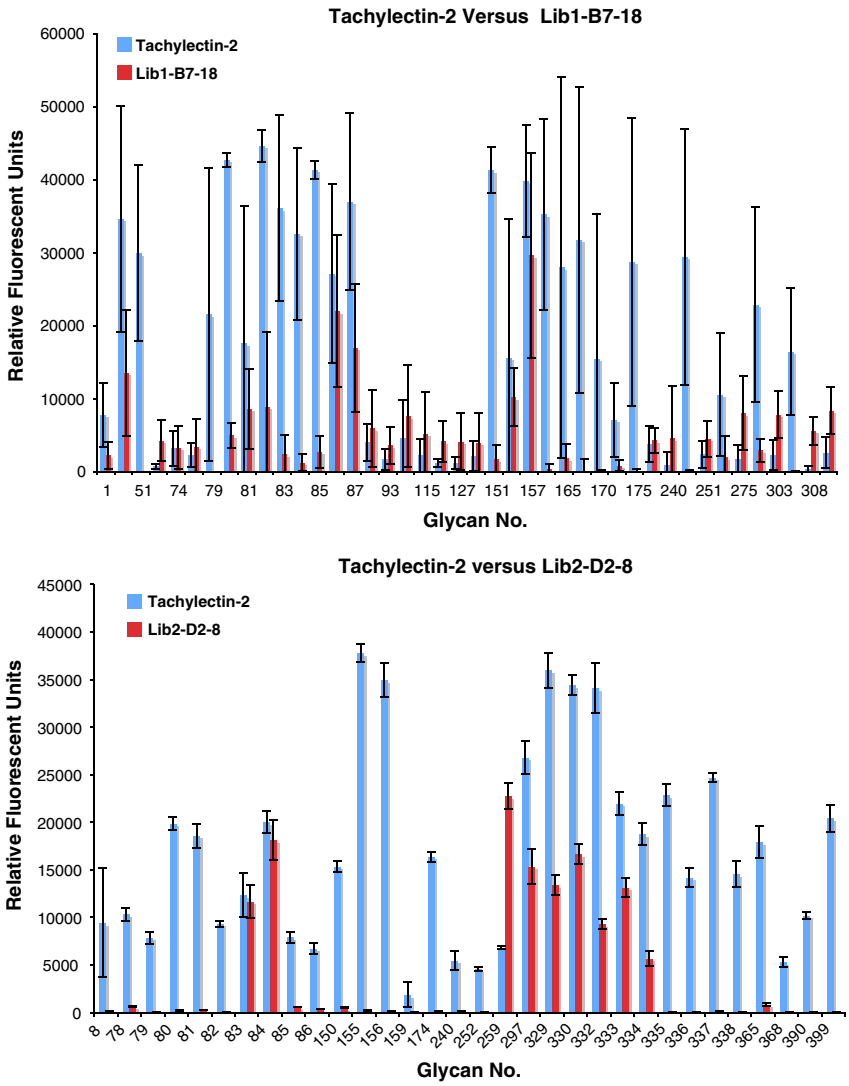

Fig. S7. Glycan array analysis of wild-type tachylectin-2 and the evolved variants. The interaction of the lectins with the array of glycans was measured by fluorescence intensity using biotin labeled lectins. Presented are the comparisons between the 25 glycans that gave the highest signals in the wild-type and/or evolved variants Lib1-B7-18 and Lib2-D2-8. The complete results including comprehensive oligosaccharide list (Plate Array Version 3 and 3.2 respectively) are available from the Consortium of Functional Glycomics (http://www.functionalglycomics.org/).

Table S1. Sequence changes in variants derived from Lib2-D2 upon directed evolution for higher foldability

Lib2-D2(Net)														
Position		3	12	23	25	26	34	35	40	48	53	55	61	77	82
Residue		Gly	Pro	Asn	Lys	Ile	His	Asp	Met	Asn	Gln	Gln	Pro	Ser	Asp
Round 1 variants *	1 (LP1G3)											Glu			
	2 (LP1B4)			Asp											
	3 (LP2H6)												Asp		
	4 (HP1A11)									Asp					
	5 (HP1G11)		Pro												
Round 2 variants	6 (LP1E5)								Leu	Asp					
	7 (LP1F6)			Asp	Asn										
	8 (LPA11)			Asp		Leu									
	9 (HP3F7)			Asp								Glu			
	10 (HP1G9)			Asp								Glu			
Round 3 variants	11 (P2H2)							Gly	Leu	Asp					Ala
	12 (P2H4)	Asp		Asp		Leu									
	13 (P1G7)			Asp		Leu	Gln	Val			Arg				
	14 (P6A9)	Asp		Asp		Leu									
	15 (P2A11) †								Leu	Asp				Pro	

*For simplicity, the evolved variants derived from the wild-type fragment Lib2-D2 were sequentially numbered as Lib2-D2-1 to Lib2-D2-15. The original annotations of these variants are given in parenthesis.

†Variant Lib2-D2-15, the structure of which is available and its complete amino acid sequence is: MGGWSNFKFLFLSPGGELYGVLNDKIYKGTPPTHDNDNWLG RAKKIGDGGWNQFQFLFFDPNGYLYAVSKDKLYKAPPPQSDTDNWIARATEIGSGG

Table S2. Summary of crystallization and data refinement

Data Collection	Lib2-D2-15	Lib1-B7-18
Resolution range (Å) *	50.0–2.5 (2.54–2.50)	50.0–2.5 (2.54–2.50)
Space group	C2	$P3_2$
Unit cell dimensions:		
a (Å)	125.56	80.56
b (Å)	56.42	80.56
c (Å)	83.30	170.68
β^o	122.9	
Number of molecules in the asymmetric unit	5	10
Number of reflections measured	55,992	264,217
Number of unique reflections *	17,718 (797)	42,804 (2111)
R_{sym} *, †	0.09 (0.39)	0.118 (0.452)
Completeness (%) *	998.9 (90.3)	99.7 (98.6)
Redundancy	3.2 (2.3)	6.2 (4.7)
$\langle I \rangle > / \langle \sigma(I) \rangle$	13.6 (2)	34.6 (4.2)
Refinement statistics		
Resolution limits (Å)	50.0–2.5	50.0–2.5
R_{free} ‡ (%)	29.9	27.0
R_{work} ‡ (%)	23.3	20.4
Mean B factor (Å^2)	37.3	36.17
rms deviations (Å)	0.012	0.025
Bond angles (°)	1.52	2.33
Torsion angles (°)	7.0	8.52
Ramachandran plot		
Most favored (%)	84.9	94.7
Additionally favored (%)	13.7	4.2
Generously allowed (%)	0.8	
Disallowed regions (%)	0.6	

*Values in parentheses are for the highest-resolution shells.

†$R_{sym} = \sum |\langle I_{hkl} \rangle - I_{hkl}| / I_{hkl}|$, where $\langle I_{hkl} \rangle$ is the average intensity over symmetry-related reflections and I_{hkl} is the observed intensity.

‡$R = \sum ||F_o| - |F_c|| / \sum |F_o|$, where F_o denotes the observed structure factor amplitude and F_c the structure factor calculated from the model.

Table S3.

	Number of sites (n)	K_a M^{-1}	ΔH cal/mole	ΔS (cal/mol)/ deg	K_a M^{-1} Fluorescence quenching /equilibrium dialysis
Lib1-B7-18(ITC)	4	$1.2 * 10^3 \pm 53$	$-3.5 * 10^3 \pm 73.4$	2.57	
Lib2-D2-15(ITC)	4	$4.3 * 10^3 \pm 302$	$-4.3 * 10^3 \pm 111$	2.2	
Tachylectin-2 (ITC)	5	$1.2 * 10^3 \pm 301$	$-1 * 10^3 \pm 136$	10.7	
Tachylectin-2 (by fluorescence quenching)					$8.3 * 10^3$ *$1.95 * 10^4$ †

*Data from ref. 10.
†Data from ref. 11.